Available online at www.sciencedirect.com
ScienceDirect
Journal of Photochemistry and Photobiology A: Chemistry 194 (2008) 297–307
Journal of Photochemistry and Photobiology A:Chemistry
www.elsevier.com/locate/jphotochem

The interaction of silibinin with human serum albumin: A spectroscopic investigation

Tushar Kanti Maiti [1], Kalyan Sundar Ghosh, Anirban Samanta, Swagata Dasgupta *

Department of Chemistry, Indian Institute of Technology, Kharagpur 721302, India

Received 24 May 2007; received in revised form 9 July 2007; accepted 28 August 2007
Available online 1 September 2007

Abstract

Silibinin is a well-known naturally occurring compound used for the treatment of a wide range of hepatitic diseases. In this study, we report the binding of silibinin to the carrier protein, human serum albumin (HSA) under physiological conditions. UV–Vis and fluorescence quenching methods in combination with Fourier transformed infrared (FT-IR) and circular dichroism (CD) spectroscopy have been used to study the nature and mode of binding. The binding parameters were determined from tryptophan fluorescence quenching by a Scatchard plot and the results were found to be consistent with those obtained from a modified Stern–Volmer equation. The association constant is of the order of 10^5. The change in enthalpy (ΔH°) and entropy (ΔS°) due to the interaction were found to be $-6.76\,\mathrm{kJ\,mol^{-1}}$ and $73.69\,\mathrm{J\,mol^{-1}\,K^{-1}}$, respectively. These values suggest that apart from an initial hydrophobic association, electrostatic interactions play a decisive role during complexation of silibinin with HSA. Observations from FT-IR and CD spectra upon ligand binding indicate changes in the secondary structure of HSA. Docking studies that corroborate our experimental results reveal that the silibinin molecule lies within hydrogen bonding distance of Trp 214 and Asp 451 residues of subdomains IIa and IIIa of HSA, respectively.

Keywords: Silibinin; Human serum albumin; Fluorescence; Fourier transformed infrared; Circular dichroism; Docking

1. Introduction

The extracts of the flowers and leaves of *Silybum marianum* (St. Mary's thistle) have been used for centuries to treat a wide range of liver and gall bladder disorders, including hepatitis, cirrhosis and jaundice, and to protect the liver against poisoning from chemical and environmental toxins. The plant extract contains a mixture named silymarin, whose main constituents are silibinin, isosilibinin, silicristin, and silidianin [1]. The chemical structure of the major constituent, silibinin (3,5,7-trihydroxy-2-[3-(*S*)-(4-hydroxy-3-methoxyphenyl)-2-(*S*)-(hydroxymethyl)-2,3-dihydro-1,4-benzodioxin-6-yl]chroman-4-one) is shown in Fig. 1A.

Recently silibinin has received attention due to its alternative beneficiary activities that are not directly related to its hepatoprotective actions [2]. It was tested for inhibition of human cytochrome P-450 enzymes by virtue of its inhibition of superoxide anion formation in stimulated neutrophils [3,4]. *In vitro* experiments demonstrated that the enzymatic activity of DNA-dependent RNA-polymerase I is stimulated by silibinin and protein biosynthesis is indirectly intensified [5]. Another promising activity of this compound is reflected in its anticancer activity that results at least partially from its cytoprotective, antioxidant, and chemopreventive properties [6]. It has also been found that the flavanolignans, such as silibinin, isosilibinin, silidianin and silicristin display very potent antioxidant and anticancer activity [7], and prevent hepatocytes from ethanol-induced damage [8]. Considering the antihepatotoxic activity of silibinin, a widely used drug and supplement for various liver disorders, together with its strong preventive and anticancer efficacy against various epithelial cancers, we considered it pertinent to investigate the binding of silibinin with human serum albumin.

Human serum albumin (HSA) is the most abundant carrier protein of the body with a high affinity for a wide range of metabolites and drugs [9]. The most important physiological role of the protein is to bring such solutes into the blood

* Corresponding author. Tel.: +91 3222 283306; fax: +91 3222 255303.
E-mail address: swagata@chem.iitkgp.ernet.in (S. Dasgupta).
[1] Present address: Department of Organic Chemistry, Weizmann Institute of Science, Rehovot 76100, Israel.

1010-6030/$ – see front matter © 2007 Elsevier B.V. All rights reserved.
doi:10.1016/j.jphotochem.2007.08.028

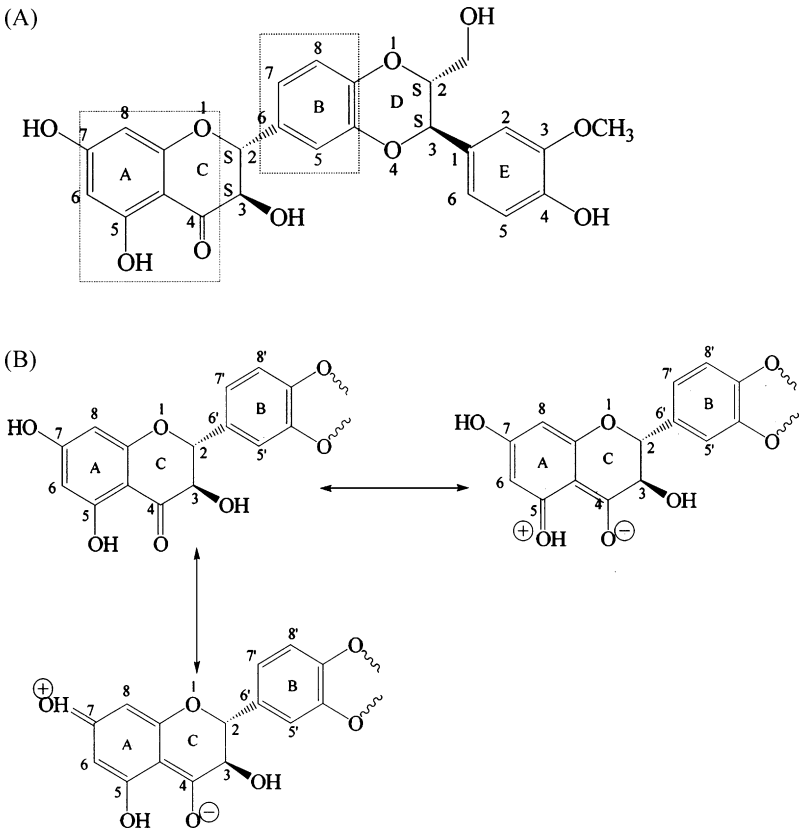

Fig. 1. (A) Chemical structure of silibinin (3,5,7-trihydroxy-2-[3-(*S*)-(4-hydroxy-3-methoxyphenyl)-2-(*S*)-(hydroxymethyl)-2,3-dihydro-1,4-benzodioxin-6-yl]chroman-4-one). (B) Mesomeric structure illustration of the excited states of silibinin.

stream and then deliver them to the target organs, as well as to maintain the pH and osmotic pressure of plasma. The molecular interactions between HSA and many compounds have been investigated successfully including many drugs [10,11]. It has recently been proved that serum albumin plays a decisive role in the transport and disposition of flavonoids like quercetin, rutin and genistein [12–14]. From this laboratory we have already reported the interaction of two naturally occurring compounds having medicinal impact namely (−)-epigallocatechin gallate and all-*trans*-retinoic acid with this protein [15,16].

The distribution and metabolism of many biologically active compounds in the body whether drugs or natural products are

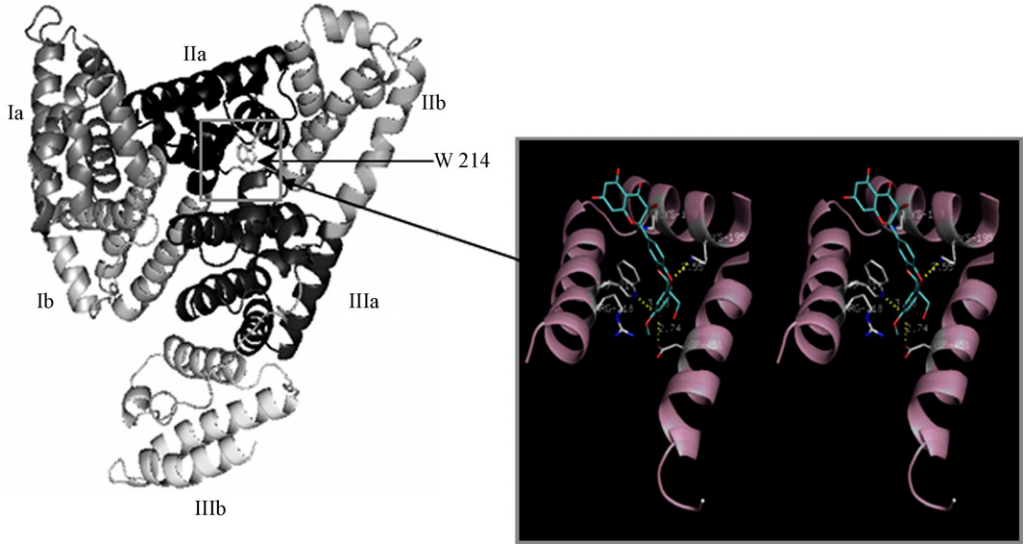

Fig. 2. Cartoon representation of human serum albumin (PDB entry 1AO6). Each subdomain has been marked and the location of Trp 214 shown. Stereoview of the docking pose of HSA and silibinin is shown in the inset and the residues within hydrogen bonding distance of silibinin are marked.

correlated with their affinities toward serum albumin. Thus, the study on the interaction of such molecules with albumin is of imperative and fundamental importance. The globular protein, HSA is composed of three structurally similar domains (I–III), each containing two subdomains (a and b) and stabilized by 17 disulfide bridges [17–19] (Fig. 2). The sole tryptophan residue (Trp 214) of HSA is in subdomain IIa. The ability of HSA to interact with many organic and inorganic molecules is attributed to the presence of multiple binding sites. This makes the protein an important regulator of intercellular fluxes that plays a major role in the pharmacokinetic behavior of many drugs [20].

In this study, we have investigated the binding of silibinin with human serum albumin to understand how these compounds can be efficiently exploited to combat diseases. We have explored the interaction of silibinin with HSA by biophysical methods mainly fluorescence, FT-IR and CD studies. Thermodynamic parameters have been calculated according to the van't Hoff equation to determine the types of interactions involved and finally we have performed docking studies to obtain a clearer insight into the residues involved in the interaction.

2. Materials and methods

2.1. Materials

Human serum albumin (fatty acid free) fraction V and silibinin were from Sigma. D_2O was from Acros Organics and all other reagents were from SRL India. All solutions were prepared in 20 mM phosphate buffer of pH 7.0. The concentration of HSA and silibinin were determined spectrophotometrically (Perkin-Elmer UV–vis spectrophotometer model Lambda 25) using ε_{280}(HSA) = 35500 M^{-1} cm^{-1} [21] and ε_{288}(silibinin) in ethanol = 21745 M^{-1} cm^{-1} [22].

2.2. Determination of association constants of HSA–silibinin complexes by UV–Vis method

Due to poor solubility of silibinin in aqueous solution, a stock solution (0.41×10^{-3} M) of silibinin was prepared in ethanol and was used by dilution with 20 mM phosphate buffer of pH 7.0 permitting a maximum alcohol concentration of ~2.5%. Finally 1×10^{-5} M silibinin solution was titrated by successive addition of 1.07×10^{-4} M HSA solution and UV–Vis spectra recorded. In order to obtain the ground state association constant, K_a for a 1:1, silibinin:HSA complex, the following equilibrium can be represented as

$$\text{silibinin} + M = \text{silibinin} - M$$

where M denotes the macromolecule (HSA). The equilibrium constant of complex formation can be estimated from the changes in absorbance at a fixed wavelength, using the Benesi–Hildebrand equation (Eq. (1)) [23]:

$$\frac{1}{\Delta A} = \frac{1}{(\varepsilon_b - \varepsilon_f)L_T} + \frac{1}{(\varepsilon_b - \varepsilon_f)L_T K_a}\frac{1}{M} \quad (1)$$

where ε is the extinction coefficient, the subscripts b, f and T denote bound, free and total ligand, L_T the total silibinin concentration, M the concentration of the macromolecule and ΔA is the change in the absorbance at a given wavelength. By plotting the reciprocal of absorbance change versus the reciprocal of concentration of the macromolecule, the association constant for complex formation (K_a) can be calculated from the ratio of the intercept to the slope.

2.3. Fluorescence spectroscopy

2.3.1. Fluorescence quenching of HSA by silibinin

Fluorescence measurements were performed using a Jobin Yvon spectrofluorimeter model Fluoromax-3 in a 1 cm quartz cell using an excitation wavelength of 295 nm. The excitation and emission bandwidths were 5 nm. The emission spectra were recorded from 310 to 450 nm. A quantitative analysis of the interaction between silibinin and HSA was performed by a fluorimetric titration of 2.5 ml solution of HSA (2.9 μM) with successive additions of 10 μl of silibinin solution (1 mM in ethanol) to reach a final concentration of silibinin of 38 μM maintaining maximum alcohol content <4%, which does not cause any structural change to the protein [24]. Thermodynamic parameters were obtained by conducting the fluorescence experiments at 293, 298, 303 and 313 K. The binding parameters for the HSA–silibinin complex have been calculated at 293, 298, 303 and 313 K from fluorescence quenching data using the procedure of Scatchard [25]. This method is based on the general equation:

$$\frac{r}{D_f} = nK - rK \quad (2)$$

where r is the number of moles of silibinin-bound per mole of protein, D_f the molar concentration of free silibinin, n the binding stoichiometry per class of binding sites, and K is the equilibrium binding constant.

Fluorescence quenching was also analyzed using the modified Stern–Volmer equation [26]:

$$\frac{F_0}{\Delta F} = \frac{1}{f_a K_a [Q]} + \frac{1}{f_a} \quad (3)$$

where $\Delta F = F_0 - F$; F_0 and F are the relative fluorescence intensities in absence and presence of the quencher, respectively, f_a the fraction of fluorophore accessible to the quencher, [Q] the concentration of quencher and K_a is the Stern–Volmer quenching constant. The plot of $F_0/\Delta F$ versus 1/[Q] yields $1/f_a$ as the intercept, and $1/(f_a K_a)$ as the slope. From the intercept and slope the values for K_a and f_a can be obtained.

Considering that the enthalpy change (ΔH°) does not vary significantly over this temperature range, ΔH° and ΔS° can be calculated using the van't Hoff equation:

$$\ln K = -\frac{\Delta H^\circ}{RT} + \frac{\Delta S^\circ}{R} \quad (4)$$

where K is the binding constant at the corresponding temperature and R is the universal gas constant. The free energy of binding is estimated from ΔH° to ΔS° values using the following relationship:

$$\Delta G^\circ = \Delta H^\circ - T\Delta S^\circ \quad (5)$$

2.3.2. Quenching studies of 8-anilino-1-naphthalene sulfonic acid (ANS)-bound HSA

Human serum albumin (2.9 μM) was saturated with ANS (9 μM) [14] in 20 mM phosphate buffer containing 50 mM NaCl (pH 7.0) and silibinin was added successively to this solution to reach a final concentration of 38 μM. The concentration of ANS was determined by its molar absorption coefficient of 4.95×10^3, at 350 nm [27]. Blank titrations with only silibinin were carried out and corrected for dilution. The excitation wavelength for ANS-bound HSA was set at 375 in which the emission maximum was observed at 468 nm.

2.4. Circular dichroism (CD) measurements

Circular dichroism measurements were made on a Jasco-810 automatic recording spectrophotometer, using 2 mm path length at 25 °C. The spectra were recorded in the range of 190–240 nm with a scan rate of 30 nm/min and a response time of 4 s. Three scans were accumulated for each spectrum. For CD studies the concentration of HSA was 1.53 μM. Two sets of HSA–silibinin complexes were prepared maintaining an HSA: silibinin molar ratio of 1:1 and 1:2, respectively. Results were expressed in terms of ellipticity and the secondary structure determined using DICHROWEB, an online server for protein secondary structure analyses from circular dichroism spectroscopic data [28].

2.5. FT-IR spectroscopic measurements

Twenty milligrams per milliliter HSA solution was prepared in 20 mM phosphate buffer of p*D* 7.2 in 99.9% D_2O giving a final concentration of 0.30 mM. Three sets of HSA–silibinin complexes were prepared by maintaining final silibinin concentrations at 0.0023, 0.023 and 0.23 mM. FT-IR measurements were carried out at room temperature on a Nexus-870 FT-IR spectrometer equipped with a germanium attenuated total reflection (ATR) accessory, a DTGS KBr detector and a KBr beam splitter. All spectra were taken by means of the Attenuated Total Reflection (ATR) method. For each spectrum, a 256-scan interferogram was collected in a single beam mode with a 4 cm^{-1} resolution. Control buffer spectra were also recorded under identical conditions. The background was corrected before every sample. The content of secondary structural elements of HSA and the HSA complexes with silibinin were obtained by the method described by Byler and Susi [29] as mentioned elsewhere [15].

2.6. Molecular docking

The crystal structure of HSA (PDB entry 1AO6) was downloaded from the Protein Data Bank [30] and used for docking studies. The 3D structure of silibinin generated in Sybyl 6.92 (Tripos Inc., St. Louis, USA) was energy-minimized with the help of the MMFF94 force field using MMFF94 charges. Waters were removed from protein PDB files, polar hydrogen atoms were added and Kollman United Atomic charges were assigned. Rotatable bonds in the ligands were assigned with Auto Dock Tools. Protein-ligand docking was carried out with the AutoDock 3.0.5 Lamarckian genetic algorithm (GA) [31]. Hundred individual GA runs were performed to generate 100 docked conformations. The protein was enclosed in a grid with dimensions 90 Å × 90 Å × 90 Å with a grid spacing of 0.3 Å. Trp 214 of the protein was taken as the center of the grid. Other miscellaneous parameters were assigned the default values given by the AutoDock program. The protein structure was kept fixed during docking. The output from AutoDock was rendered with PyMol [32].

The accessible surface area of HSA (uncomplexed) and the HSA–silibinin docked complex were calculated using NACCESS [33]. The structure of silibinin corresponding to the final docked conformation was chosen and composite coordinates were generated to form the docked complex. The change in accessible surface area (ΔASA) was calculated using the expression $\Delta ASA^i = ASA^i_{HSA} - ASA^i_{HSA-silibinin}$. In this case if a residue lost more than 20 $Å^2$ ASA when going from the uncomplexed to the complexed state it was considered as being involved in the interaction.

3. Results and discussion

3.1. UV studies

The interaction of silibinin with HSA has been studied by UV–Vis, fluorescence, CD and FT-IR spectroscopy followed by docking studies to gain an insight into the mode of binding of this molecule with the most abundant carrier protein. In the spectral range from 240 to 400 nm, dihydroflavonols show two major absorption bands: band I (300–400 nm) and band II (240–280 nm) [34]. Band I originates due to light absorption of the A + C rings and corresponds to a π–π* transition which can be represented by the two resonance structures shown in Fig. 1B [35]; band II is due to the absorption of the B ring (Fig. 1). The zwitterionic or charge separated forms represent the excited states and both the transitions are electronically allowed. Similar types of bands are also observed for flavones like quercetin [36]. The characteristic features of silibinin are observed in the spectrum marked (i) in Fig. 3 in phosphate buffer pH 7.0 containing 2.5% ethanol. Spectra of HSA-bound silibinin (silibinin–HSA complex minus HSA alone) are shown in Fig. 3 together with the spectrum of silibinin alone having the same concentration. On binding of protein, a bathochromic shift is observed in band I (8 nm), which indicates the presence of a specific interaction between the ligand and its binding environment. The most acidic phenolic OH groups of silibinin are in the 3′, 7′ and 2′ positions [34,37], which are dissociated at physiological pH. The process being incomplete results in a mixture of neutral and anionic species. The involvements of phenolic OH substituents of ring A (either 5 or 7 or both) leads to a bathochromic shift due to extensive π conjugation and deprotonation of phenolic OH substituents. The slight band broadening of band I of silibinin can be attributed to specific, noncovalent interactions with amino acid residues of the binding site. The two isobestic points at 291 and 311 nm are indicative of the occurrence two consecutive equilibria during complex formation. The association constant

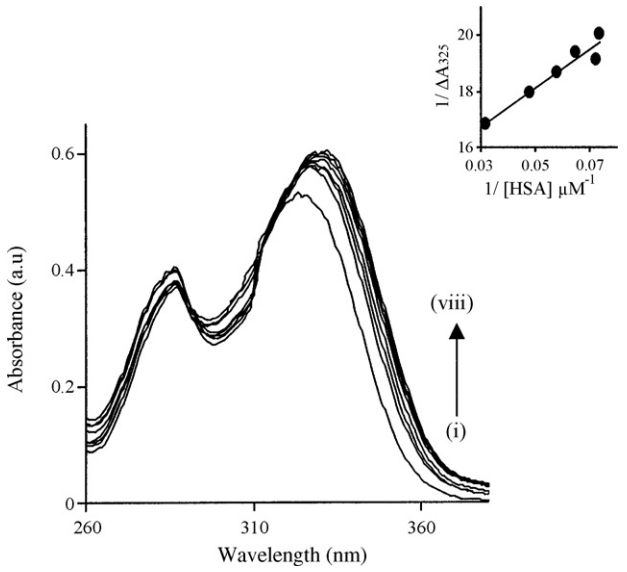

Fig. 3. UV–Vis spectra of silibinin (1×10^{-5} M) in 20 mM phosphate buffer of pH 7.0 containing 2.5% ethanol marked as (i). Spectra of HSA-bound silibinin (slibinin–HSA complex minus HSA alone) are shown from (ii) to (viii). Inset: Benesi–Hildebrand plot.

value obtained from UV studies using the Benesi–Hildebrand equation [23] is 2.11×10^5 M^{-1} (Fig. 3 inset).

3.2. Fluorescence studies

3.2.1. Quenching of HSA by silibinin

The gradual decrease in fluorescence intensity of HSA on addition of silibinin indicates that there exists an interaction between the protein and ligand. The ligand being nonfluorescent under the experimental conditions, the strong fluorescence emission of HSA at 347 nm is attributed to its single tryptophan residue (Trp 214). The decrease in fluorescence intensity observed on ligand binding is accompanied by a red shift from 347 to 356 nm on addition of silibinin. One representative fluorescence titration spectra at 293 K is shown in Fig. 4A, the inset shows the shift of λ_{max} with increasing concentration of the ligand. The results indicate that there is a shift of the sole tryptophan residue to a more polar environment on ligand binding.

The association constants, K and binding stoichiometry, n for the HSA–silibinin complex at 293, 298, 303 and 313 K were calculated from a Scatchard plot (Fig. 6). From the modified Stern–Volmer plot shown in Fig. 7, the fractional accessibility of Trp 214 that is accessible to the quencher was calculated. The mean fractional accessibility of Trp over the temperature range is 1.02 ± 0.02. This implies that silibinin easily enters the hydrophobic cavity of subdomain IIa. The binding parameters at the four different temperatures for the HSA–silibinin interaction were calculated from the Stern–Volmer plot and Scatchard plots and are shown in Table 1. The mean values for the binding parameters are $1.13 \pm 0.18 \times 10^5$ and $0.98 \pm 0.02 \times 10^5$ M^{-1}, respectively. The linear Scatchard plots indicate that silibinin binds to a single class of sites on HSA, which is in agreement with the number of binding sites n. The binding constants are

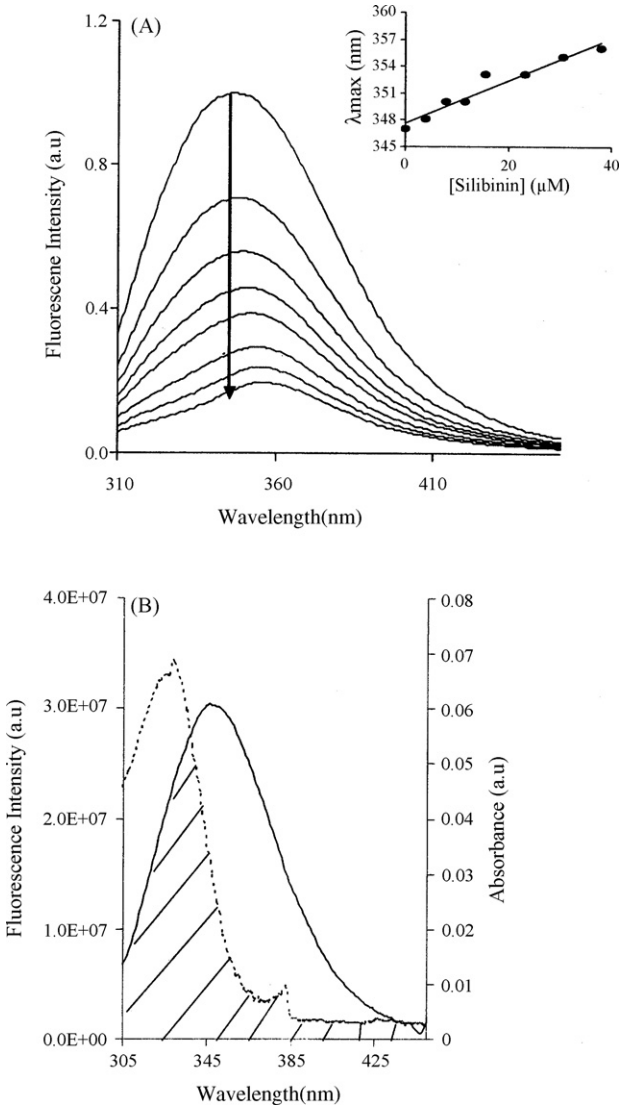

Fig. 4. (A) Fluorescence spectra of the HSA–silibinin system. The concentration of HSA was 2.89 μM and silibinin concentration increased from 0 to 3.79×10^{-5} M. $T = 293$ K; pH 7.0; $\lambda_{ex} = 295$ nm. Arrow indicates the increase in silibinin concentration. Inset: shift of λ_{max} of emission with increase in silibinin concentration. (B) Spectral overlap between the fluorescence emission spectrum of HSA (solid line) and UV absorption spectrum of silibinin (dotted line) in phosphate buffer pH 7.0. [silibinin]/[HSA] = 1:1; $\lambda_{ex} = 295$ nm; $\lambda_{em} = 347$ nm.

found to decrease with increase in temperature suggesting the involvement of noncovalent interactions in the binding of silibinin to HSA. The association constant value obtained from the fluorescence experiment is concurrent with the value obtained from UV studies.

3.2.2. ANS binding studies

ANS, known to bind to hydrophobic pockets of proteins, is a much-utilized fluorescent 'hydrophobic probe' used primarily to examine the nonpolar character of proteins and membranes [38]. ANS binds in the hydrophobic subdomains (IIa and IIIa) of HSA [14]. The replacement of ANS by silibinin in the protein indicates that ANS and silibinin bind to the same site. This is

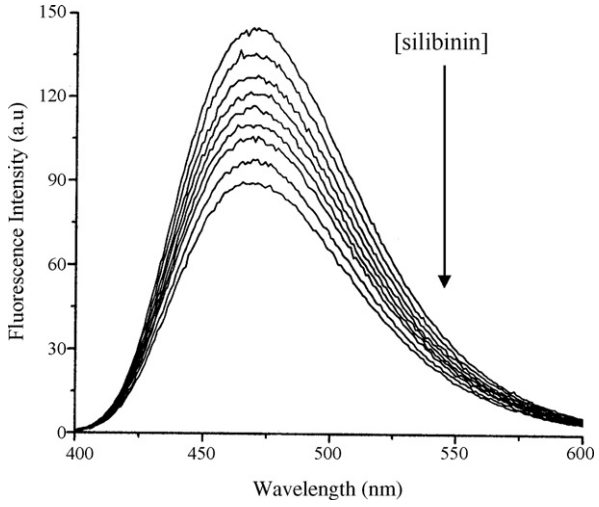

Fig. 5. Fluorescence quenching spectra of ANS-bound HSA in absence (top) and presence of silibinin in phosphate buffer pH 7.0. [HSA] = 2.9 μM; [ANS] = 9 μM; silibinin concentration varied from 0 to 38 μM; λ_{ex} = 375 nm; λ_{em} = 468 nm.

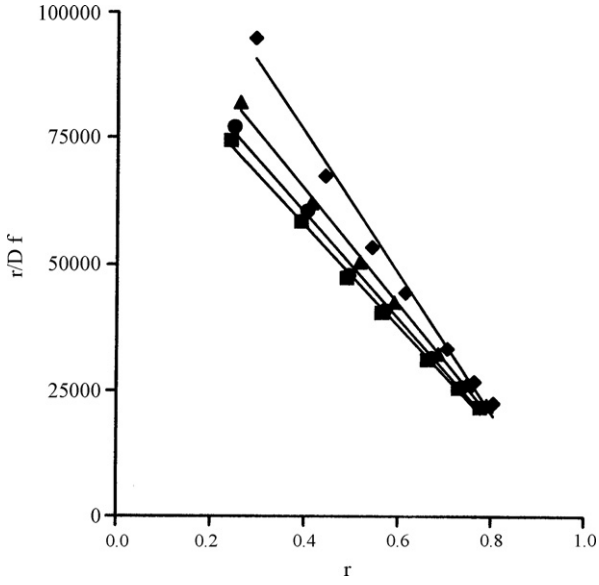

Fig. 6. Scatchard plot for the HSA–silibinin system at pH 7.0. HSA concentration: 2.89 μM; (♦) 293 K; (■) 298 K; (▲) 308 K; (●) 313 K; λ_{ex} 295 nm.

corroborated by the decrease in ANS-bound HSA fluorescence with increasing concentrations of silibinin (Fig. 5), which confirms the accessibility of hydrophobic pocket (IIa and/or IIIa) of HSA by silibinin.

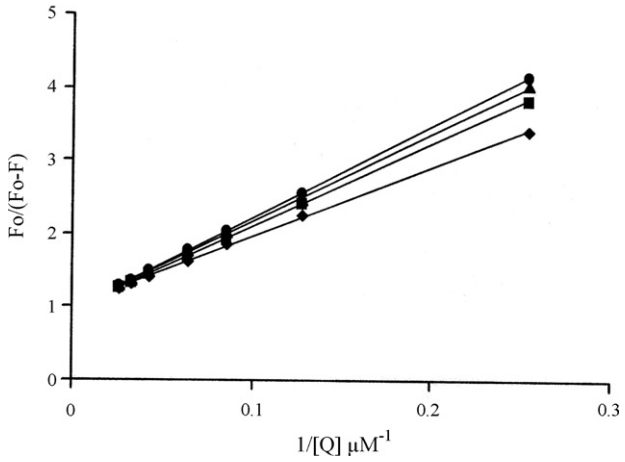

Fig. 7. Modified Stern–Volmer plots of the HSA–silibinin system. HSA concentration: 2.89 × 10^{-6}; pH 7.0; (♦) 293 K; (■) 298 K; (▲) 308 K; (●) 313 K; λ_{ex} 295 nm.

3.2.3. Energy transfer and binding distance between HSA and silibinin

The spectral overlap between the fluorescence emission spectrum of HSA and the UV absorption spectrum of silibinin after binding indicates the possibility of energy transfer. Fluorescence resonance energy transfer is an electrodynamic phenomenon, which occurs between a donor molecule in the excited state and an acceptor molecule in the ground state and does not involve any emission or reabsorption of photons. This non-radiative energy transfer largely depends on the donor–acceptor distance (Förster distance) [26]. According to Förster's energy transfer theory [26], the efficiency of energy transfer, E, can be calculated using the following equation:

$$E = 1 - \frac{F}{F_0} = \frac{R_0^6}{R_0^6 + r^6} \quad (6)$$

where F and F_0 are the fluorescence intensities of HSA in the presence and absence of silibinin, r the distance between acceptor and donor and R_0 is the critical distance when the energy transfer efficiency is 50%. The value of R_0 is calculated using the following equation [26]:

$$R_0(\text{Å}) = 9.78 \times 10^3 [(\kappa^2 n^{-4} Q_D J(\lambda)]^{1/6} \quad (7)$$

where κ^2 is the relative orientation in space of the transition dipoles of the donor and acceptor, n the refractive index of the medium, Q_D the fluorescence quantum yield of the donor in absence of acceptor and J is the overlap integral of the fluorescence emission spectrum of the donor and the absorption

Table 1
Thermodynamic parameters for silibinin binding to HSA

Temp. (K)	K_a (×10^5 M^{-1})		n	ΔG° (kJ mol^{-1})	ΔH° (kJ mol^{-1})	ΔS° (J mol^{-1} K^{-1})
	Stern–Volmer	Scatchard method				
293	1.012	1.386	0.95	−28.35	−6.76	73.69
298	0.972	1.121	0.97	−28.72		
303	0.970	1.037	0.98	−29.09		
313	0.965	0.986	0.98	−29.83		

spectrum of the acceptor. J was calculated from the following equation [26]:

$$J = \frac{\int F_D(\lambda)\varepsilon_A(\lambda)\lambda^4\,d\lambda}{\int F_D(\lambda)\,d\lambda} \quad (8)$$

where F_D (λ) is dimensionless and is the corrected fluorescence intensity of the donor in the wavelength range λ–$\lambda + \Delta\lambda$ with the total intensity (area under the curve) normalized to unity. $\varepsilon_A(\lambda)$ is the extinction coefficient of the acceptor at λ, which is typically in the units of $M^{-1}\,cm^{-1}$.

J was calculated by integrating the overlap area of the spectrum shown in Fig. 4B with Origin 6.0, from 305 to 450 nm—the value obtained was $1.27 \times 10^{-14}\,M^{-1}\,cm^3$. By using, $\kappa^2 = 2/3$, $n = 1.336$ and $Q_D = 0.118$ [39,40], R_0 was calculated from Eq. (7) and was found to be 2.53 nm. The value of r was 3.0 nm from Eq. (6) using $E = 0.107$. The donor-to-acceptor distance lies within the range of 0.5–2 R_0 [26], indicative of an efficient energy transfer from HSA to silibinin.

3.3. Circular dichroism studies

The CD spectrum of HSA exhibits two negative bands in the ultraviolet region at 209 and 221 nm as shown in Fig. 8. This is characteristic of the α-helical structure of a protein. The secondary structure was determined using CDSSTR method in DICHROWEB, an online server for protein secondary structure analysis. By this method it was found that the α-helical content of the protein changed from 54 to 52% upon binding with silibinin. There is a negligible difference in β-sheet content from 20 to 21% and the unordered structure of the protein remains almost unaltered due to interaction. From the above CD analysis, it is observed that the interaction of HSA with silibinin at a molar ratio 1:2 causes a slight loss in its helical content. To know whether the binding of HSA to silibinin causes any conformational change of the ligand, we have also checked the CD of silibinin in presence and absence of protein. However, no protein-induced CD change was observed.

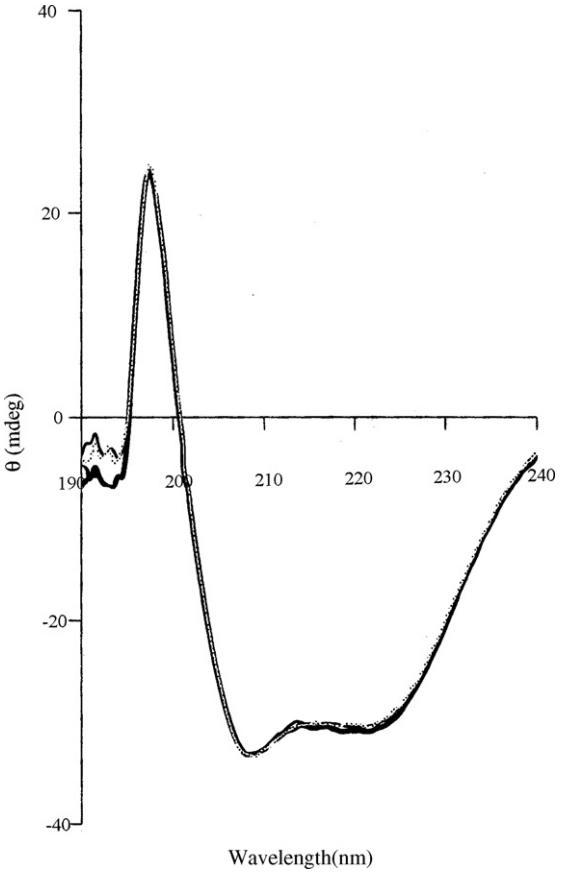

Fig. 8. CD spectra of HSA–silibinin complexes at pH 7.0. HSA (1.53 μM) (thick line); 1:1 HSA and silibinin (dot); 1:2 HSA and silibinin (thin line).

3.4. FT-IR studies

The protein amide I band at 1650–1654 cm^{-1} (mainly due to C=O stretching) and amide II band at 1548–1560 cm^{-1} (C–N stretch coupled with N–H bending mode) are related to the secondary structure of proteins [29]. The key factors known to govern the conformational sensitivity of the amide bands in proteins are hydrogen bonding and the coupling between transition dipoles. Difference spectra also provide information about the conformational changes that arise due to complex formation. Fig. 9 represents the FT-IR spectra before and after binding of silibinin to HSA for varying concentrations of silibinin. The amide I peak position shifts from 1652 cm^{-1} (free HSA) to 1648 cm^{-1} (HSA–silibinin complex). This implies that the secondary structure of the protein is affected on complex formation. A quantitative analysis of this change is presented later. In the amide II region, the peaks at 1532, 1549, 1569, 1582 cm^{-1} of free HSA show a slight shift on complexation. The shift observed in the peak at 1444 cm^{-1} arises due to (i) CH_2 and CH_3 bending modes of the side chains and (ii) bending modes of traces of

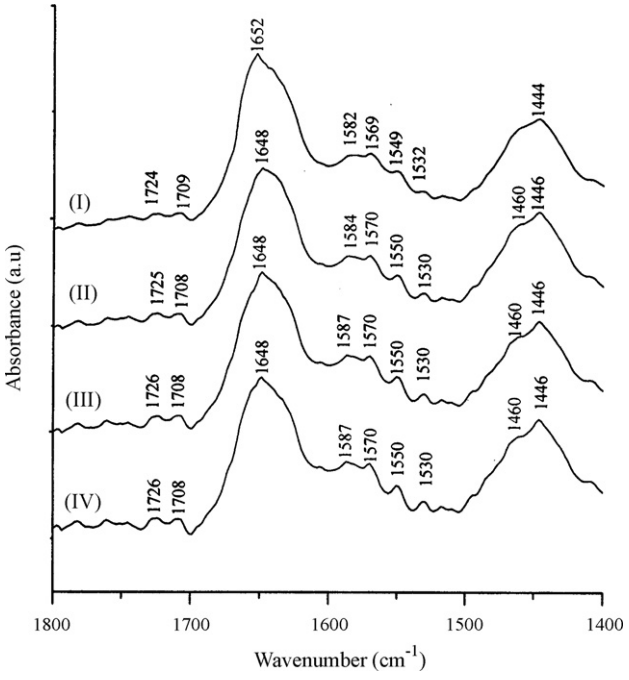

Fig. 9. FT-IR spectra of HSA (I) and HSA-bound to silibinin (II–IV).

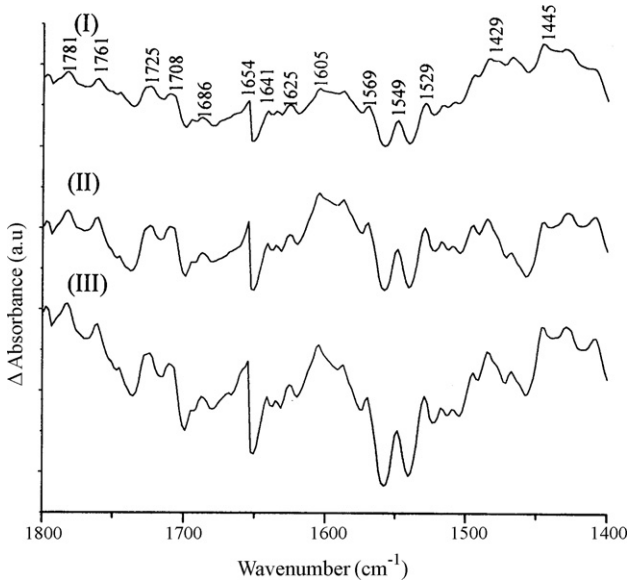

Fig. 10. FT-IR difference spectra [(HSA solution + silibinin solution) − (HSA solution)] for HSA–silibinin complexes. HSA concentration: 0.3 mM and silibinin concentrations (0.0023 mM, 0.023 mM, 0.23 mM, respectively for I, II, III).

HOD [41,42]. The bands appearing near 1444 and 1460 cm^{-1}, however, are not involved in the secondary structure calculations of either the protein or the protein–silibinin complex.

The difference spectra of the interaction of HSA with three different concentrations of silibinin are shown in Fig. 10. At low silibinin concentration (2.3 μM), positive peaks appear at 1654, 1641 and 1625 cm^{-1} (amide I) and 1569, 1549 and 1529 cm^{-1} (amide II). The negative features observed in the amide I and amide II bands indicate that silibinin is hydrogen bonded with the C=O and C–N groups of the protein polypeptide chain. In general, the spectral ranges from 1610 to 1632 cm^{-1}, 1636 to 1644 cm^{-1}, 1650 to 1662 cm^{-1} and 1665 to 1680 cm^{-1} in the amide I region are attributed to β-sheet, random coil, α-helix and turn structures, respectively [42,43]. As shown in Fig. 10, the maximum change in amide I band is in the α-helical region after interaction with silibinin. This indicates that the α-helix conformation of HSA is perturbed due to the interaction of silibinin with HSA. As the concentration of silibinin is increased 10-fold to 23 μM (Fig. 10(II)) and 100-fold (Fig. 10(III)), there is an enhancement in the intensity of each peak without any change in peak positions.

The effects on the secondary structure are more prominent in the deconvoluted spectra of HSA and the HSA–silibinin complex (Fig. 11). The free protein contained 59% α-helix, 28% β-sheet, 8% random structure, 6% turn. The estimated content of different secondary structures in native HSA is consistent with those already reported in literature [15,44–46]. On interaction of silibinin with HSA, the α-helix content was reduced from 59 to 54%. A reduction in the α-helical content was also obtained from CD studies as discussed earlier. The β-sheet content increased from 28 to 35%. The random structure content remains same whereas turn structure decreased from 6 to 2% at the highest concentration of silibinin. A similar change in the β-sheet content of HSA was also observed in the interaction with (−)-epigallocatechin gallate and polyethylene glycol [15,45]. The trend of changes in secondary structures by CD and FT-IR are similar though the content of secondary structural elements differs as discussed below. Apart from differences in sample preparation for the two methods, where a hydrated film was used for FT-IR and an aqueous solution was used for CD measurements, a major difference lies in the spectroscopic signals themselves. FT-IR signals arise from the vibrational modes whereas CD spectra are obtained from electronic transitions that may be the cause for the difference in content of their structural information. Similar differences between FT-IR and CD spectroscopic results for ribonuclease A have been reported elsewhere [47,48].

3.5. Mode of binding from thermodynamic parameters

Hydrogen bonds, van der Waals forces, hydrophobic and electrostatic interactions are primarily responsible for molecular recognition processes such as in protein-ligand binding [49]. Thermodynamic parameters, free energy (ΔG°), enthalpy (ΔH°) and entropy (ΔS°) due to complex formation provide an insight into the binding mode. To achieve this, the temperature dependence of the binding constants was studied. Experiments

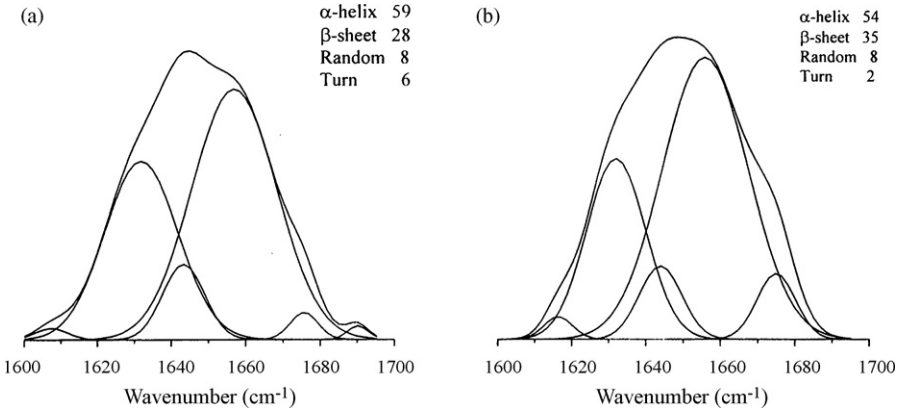

Fig. 11. Curve-fitted amide I (1700–1600 cm^{-1}) region of (a) free HSA and (b) HSA–silibinin complex in 20 mM phosphate buffer of p*D* 7.2.

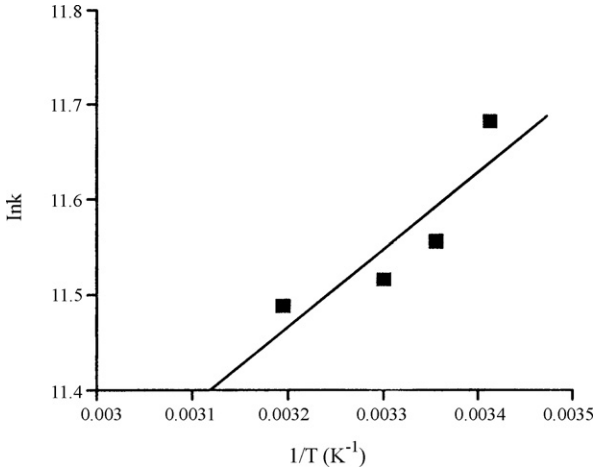

Fig. 12. van't Hoff plot of the temperature dependence of the binding constant.

were carried out at 293, 303, 308 and 313 K since HSA does not undergo any gross structural change in this temperature range [50]. From the temperature dependence of the binding constant given by the van't Hoff equation, it is possible to calculate the thermodynamic functions involved in the binding process. The binding parameters of the HSA–silibinin complex at the four temperatures were estimated from a van't Hoff plot (Fig. 12). The mean K values obtained from the Stern–Volmer equation and the Scatchard plot were used to plot the data according to Eq. (4) in Section 2. A least square regression line fitted to the data gave an R^2 value of 0.8. The ΔH° and ΔS° values were obtained from the slope and intercept, respectively.

From Table 1 it is observed that the formation of the HSA–silibinin complex is a spontaneous process with a ΔG° value of $-28.99 \pm 0.63\,\mathrm{kJ\,mol^{-1}}$. The net ΔG° for the association is essentially determined by the relative magnitude of ΔS° and ΔH° [51]. The binding of silibinin to HSA is accompanied by a negative enthalpy change ($\Delta H^\circ = -6.76\,\mathrm{kJ\,mol^{-1}}$) and a positive entropy change ($\Delta S^\circ = 73.69\,\mathrm{J\,mol^{-1}\,K^{-1}}$). This indicates that the binding is primarily due to electrostatic interactions [51]. The partial immobilization of the protein and the ligand occurs in an initial step involving hydrophobic association that results in a positive ΔS° [51]. In the subsequent interacting complex, the negative ΔH° contribution to the overall ΔG° may be associated with van der Waals interactions and hydrogen bonding.

3.6. Docking studies

Docking experiments where silibinin was docked to HSA to determine the preferred binding region within the protein molecule substantiated the results obtained from spectroscopic studies. The stereoview of the docking pose of silibinin with HSA is shown in Fig. 2. It shows that silibinin is best docked within the binding pocket of subdomains IIa and IIIa. Trp 214 is part of helix 2 of subdomain IIa (represented as IIa-h2) that spans residues 208–223. We find that in the docked conformation, the hydroxyl groups of ring A (5-OH) and E (4-OH, only one OH in E) of silibinin are within hydrogen bonding distance of (i) Tyr 150 of Ib-h3, (ii) Trp 214 of IIa-h2 and (iii) Asp 451 of IIIa-h4. The distances are given in Table 2. The involvement of ring A could explain the observed bathochromic shift and band broadening of band I of silibinin as discussed earlier. Docking of silibinin creates a hydrophilic environment near Trp 214, which may be the reason for the large red shift observed in the fluorescence spectra on binding of silibinin.

Table 2
Distances (in Å) between polar neighbors of HSA (PDB code 1AO6) and silibinin

HSA	Silibinin
Tyr 150 Oη	2.77 [C(4-O)], 2.69 [A(5-O)]
Lys 195 Nξ	2.55 [D(1-O)]
Trp 214 Nε1	3.08 [E(4-O)]
His 242 Nε2	2.61 [C(4-O)]
Asp 451 Oδ1	3.27 [E(3-O)]
Asp 451 Oδ2	3.43 [E(3-O)]
	2.74 [E(4-O)]

To further identify the residues taking part in the interaction, we calculated the accessible surface area for HSA and the HSA–silibinin complex. Residues where the absolute accessible surface areas have decreased by more than 20 Å^2 on complex formation are given in Table 3. We find that most of the residues involved in the interaction belong to subdomains IIa and IIIa as expected from our experimental results. The inside wall of the pocket of subdomain IIa which comprises site I is predominantly hydrophobic in nature with the entrance surrounded by positively charged residues such as Lys 195, Lys 199, Arg 218, Arg 222, His 242 and Arg 257. It is observed that Lys 195 loses the maximum surface area on binding (51 Å^2). Interestingly, apart from Asp 251 that loses 93% of the ASA on complex formation, Leu 238 and Ala 291 lose 86 and 100% of their ASA, respectively. This observation is in support of the thermodynamic parameters where an initial hydrophobic association has been speculated based on the ΔS° value. The subsequent hydrophilic interactions in the complex involve the polar residues. The docking studies together with the calculation of the accessible surface area on complex formation provide some insight into the mode of binding of silibinin with HSA.

Table 3
The accessible surface area (ASA) of HSA (uncomplexed) and the HSA–silibinin docked complex

Residue	ASA		ΔASA (Å^2)	Location
	(Å^2) (HSA)	(Å^2) (HSA–silibinin)		
Lys 195	91.36	39.60	51.76	Ib-h4
Lys 199	32.01	6.58	25.43	IIa-h1
Trp 214	61.74	25.42	36.32	IIa-h2
Arg 218	41.96	18.94	23.02	IIa-h2
Arg 222	37.12	9.39	27.73	IIa-h2
Leu 238	30.64	4.39	26.25	IIa-h3
Ala 291	36.99	0.00	36.99	IIa-h6
Asp 451	30.24	2.13	28.11	IIIa-h4

3.7. Determination of binding pocket

Crystal structure analyses have indicated that the principal regions of ligand binding sites of HSA are located in hydrophobic cavities in subdomains IIa and IIIa, and the sole tryptophan residue (Trp 214) is in subdomain IIa [18]. The accessibility of hydrophobic pocket (IIa and/or IIIa) was confirmed from the ANS displacement experiment. The fluorescence property of HSA is mainly due to the fluorophore Trp 214 in subdomain IIa. Thus the access to pocket IIa can be examined by monitoring the intrinsic fluorescence of Trp 214. Here the quenching of intrinsic fluorescence intensity of Trp 214 by silibinin confirms that it does bind to subdomain IIa. This is further supported by docking studies (discussed above) where Trp 214 is within hydrogen bonding distance of silibinin. This substantiates the closeness of silibinin to subdomain IIa. Finally as a part of the quenching mechanism, the spectral overlap observed makes FRET possible from the fluorophore, Trp 214 to silibinin within the characteristic Förster distance and hence confirms the binding of silibinin in subdomain IIa.

4. Conclusions

The use of naturally occurring products for the development of small molecules as potential pharmaceutical agents target human serum albumin, the most abundant carrier protein. In this report, we have studied the complex formed between silibinin and human serum albumin. The interactions have been investigated spectroscopically and theoretically by docking methods. We find that the binding constants obtained from a Scatchard plot and the Stern–Volmer equation are in the 10^5 range, with a binding stoichiometry of 1. The studies with CD and FT-IR-related to the secondary structural changes on complex formation corroborate each other indicating a slight reduction in the α-helix content. Thermodynamic parameters obtained from a van't Hoff plot indicate an initial hydrophobic association followed by electrostatic interactions. This is largely supported by the ANS binding studies where the silibinin molecule is found to displace ANS and also quench the fluorescence of Trp 214 indicating its proximity to this residue which is in subdomain IIa. FRET calculations based on the observed spectral overlap reveal a donor to acceptor distance of 3 nm indicative of efficient energy transfer. Docking studies substantiate the binding modes obtained from the experimental studies and the change in residue ASAs give some insight into the residues involved in the interactions. This study is expected to provide guidelines into understanding how silibinin with its multifarious biological potential may be further developed as a pharmaceutical agent.

Acknowledgements

SDG is grateful to Department of Science and Technology (DST), Government of India for partial financial support. The authors are also thankful to Saha Institute of Nuclear Physics, Kolkata and Central Research Facility, IIT Kharagpur for providing experimental facilities. TKM and AS thank CSIR, New Delhi for fellowships.

References

[1] A. Pelter, R. Hänsel, Tetrahedron Lett. 9 (1968) 2911–2916.
[2] S. Beckmann-Knopp, S. Rietbrock, R. Weyhenmeyer, R.H. Böcker, K.T. Beckurts, W. Lang, M. Hunz, U. Fuhr, Pharmacol. Toxicol. 86 (2000) 250–256.
[3] R. Zuber, M. Modrianský, Z. Dvoøák, P. Rohovský, J. Ulrichová, V. Šimánek, P. Anzenbacher, Phytother. Res. 16 (2002) 632–638.
[4] Z. Varga, A. Czompa, G. Kakuk, S. Antus, Phytother. Res. 15 (2001) 608–612.
[5] F. Machicao, J. Sonnenbichler, Z. Hoppe Seyler's, Physiol. Chem. 358 (1977) 141–147.
[6] E.J. Ladas, K.M. Kelly, J. Altern. Complement. Med. 9 (2003) 411–416.
[7] X. Zi, A.W. Grasso, H.J. Kung, R.A. Agarwal, Cancer Res. 58 (1998) 1920–1929.
[8] J.F. van Pelt, C. Verslype, T. Crabbe, Z. Zaman, J. Fevery, Alcohol Alcohol 38 (2003) 411–414.
[9] W.E. Muller, U. Wollert, Pharmacology 19 (1979) 56–59.
[10] Y.V. Il'ichev, L.P. Jennifer, D.S. John, J. Phys. Chem. B 106 (2002) 452–459.
[11] F. Moreno, J. Gonza'lez-Jime'nez, J. Chem. Biol. Interact. 121 (1999) 237–252.
[12] B. Sengupta, P.K. Sengupta, Biochem. Biophys. Res. Commun. 299 (2002) 400–403.
[13] O. Dangles, C. Dufour, C. Manach, C. Morand, C. Remesy, Methods Enzymol. 335 (2001) 319–333.
[14] H.G. Mahesha, S.A. Singh, N. Srinivasan, A.G.A. Rao, FEBS J. 273 (2006) 451–467.
[15] T.K. Maiti, K.S. Ghosh, S. Dasgupta, Proteins 64 (2006) 355–362.
[16] T.K. Maiti, K.S. Ghosh, J. Debnath, S. Dasgupta, Int. J. Biol. Macromol. 38 (2006) 197–202.
[17] D.C. Carter, J.X. Ho, Adv. Protein Chem. 45 (1994) 153–203.
[18] I. Petitpas, A.A. Bhattacharya, S. Twine, M. East, S. Curry, J. Biol. Chem. 276 (2001) 22804–22809.
[19] I. Petitpas, T. Grune, A.A. Bhattacharya, S. Curry, J. Mol. Biol. 314 (2001) 955–960.
[20] T. Peters Jr., Adv. Protein Chem. 37 (1985) 161–242.
[21] J. Gonza'lez-Jime'nez, G. Frutos, I. Cayre, M. Cortijo, Biochimie 73 (1991) 551–556.
[22] C. Lan, Z. Kang, S. Zhang, Z. Wu, R. Yu, Nanjing Yaoxueyuan Xuebao 21 (1983) 75–76.
[23] H.A. Benesi, J.H. Hildebrand, J. Am. Chem. Soc. 71 (1949) 2703–2707.
[24] S. Lin, M. Li, Y. Wei, Spectrochim. Acta A 60 (2004) 3107–3111.
[25] G. Scatchard, Ann. N.Y. Acad. Sci. 51 (1949) 660–673.
[26] J.R. Lakowicz, Principles of Fluorescence Spectroscopy, Springer, New York, 2006.
[27] G. Weber, L.B. Young, J. Biol. Chem. 239 (1964) 1415–1423.
[28] L. Whitmore, B.A. Wallace, Nucleic Acids Res. 32 (2004) W668–W673.
[29] D.M. Byler, H. Susi, Biopolymers 25 (1986) 469–487.
[30] M. Berman, J. Westbrook, Z. Feng, G. Gilliland, T.N. Bhat, H. Weissig, I.N. Shindyalov, P.E. Bourne, Nucleic Acids Res. 28 (2000) 235–242.
[31] G.M. Morris, D.S. Goodsell, R.S. Halliday, R. Huey, W.E. Hart, R.K. Belew, A.J. Olson, J. Comp. Chem. 19 (1998) 1639–1662.
[32] W.L. DeLano, The PyMOL Molecular Graphics System, DeLano Scientific, San Carlos, CA, USA, 2004, http://www.pymol.org.
[33] S.J. Hubbard, J.M. Thornton, 'NACCESS'. Computer Program, Department of Biochemistry and Molecular Biology, University College, London, 1993.
[34] T.J. Mabry, K.R. Markham, M.B. Thomas, The Systematic Identification of Flavonoids, Springer-Verlag, New York, 1970.
[35] S.KK. Jatkar, B.N. Mattoo, J. Ind. Chem. Soc. 33 (1956) 651–652.
[36] F. Zsila, Z. Bikádi, M. Simonyi, Biochem. Pharmacol. 65 (2003) 447–456.
[37] P.M. Agrawal, H.J. Schneider, Tetrahedron Lett. 24 (1983) 177–180.
[38] D. Matulis, R. Lovrien, Biophys. J. 74 (1998) 422–429.
[39] J.M. Vanderkooi, A. Ierokomas, H. Nakmura, A. Martonosi, Biochemistry 16 (1977) 1262–1267.

[40] L. Cyril, J.K. Earl, W.M. Sperry, Biochemists Handbook, E & EN, Spon, London, 1961.
[41] H. Susi, D.M. Byler, Biochem. Biophys. Res. Commun. 115 (1983) 391–397.
[42] H. Susi, D.M. Byler, Methods Enzymol. 130 (1986) 290–311.
[43] A.C. Dong, P. Huang, W.S. Caughey, Biochemistry 29 (1990) 3303–3308.
[44] C.N. N'soukpoé-Kossi, R. Sedaghat-Herati, C. Ragi, S. Hotchandani, H.A. Tajmir-Riahi, Int. J. Biol. Macromol. 40 (2007) 484–490.
[45] C. Ragi, M.R. Sedaghat-Herati, A.A. Ouameur, H.A. Tajmir-Riahi, Biopolymers 78 (2005) 231–236.
[46] C.N. N'soukpoé-Kossi, C. St-Louis, M. Beauregard, M. Subirade, R. Carpentier, S. Hotchandani, H.A. Tajmir-Riahi, J. Biomol. Struct. Dyn. 24 (2006) 277–283.
[47] S. Gaudreau, A. Novetta-dellen, J.F. Neault, S. Diamantoglou, H.A. Tajmir-Riahi, Biopolymers 72 (2003) 435–441.
[48] S. Seshardi, K.A. Oberg, A.L. Fink, Biochemistry 33 (1994) 1351–1355.
[49] S.N. Timaseff, in: H. Peeters (Ed.), Proteins of Biological Fluids, Pergamon Press, Oxford, 1972, pp. 511–519.
[50] S. Wang, S. Lin, M. Li, Y. Wei, T. Hsieh, Biophys. Chem. 114 (2005) 205–212.
[51] P.D. Ross, S. Subramanian, Biochemistry 20 (1981) 3096–3102.